RSC Advances

PAPER

View Article Online
View Journal | View Issue

Cite this: *RSC Adv.*, 2018, **8**, 22786

A highly selective fluorescent probe for detection of Cd^{2+} and HSO_3^- based on photochromic diarylethene with a triazole-bridged coumarin-quinoline group

Shuli Guo, Gang Liu,* Congbin Fan and Shouzhi Pu*

Received 22nd April 2018
Accepted 8th June 2018

DOI: 10.1039/c8ra03443e

rsc.li/rsc-advances

A novel photochromic diarylethene containing a quinoline-linked 3-aminocoumarin Schiff base unit (**1O**) was synthesized and used for the selective detection of Cd^{2+} and HSO_3^-. The synthesized probe exhibited a straightforward response for the selective detection of Cd^{2+}. Its fluorescence emission red-shifted ~126 nm and was enhanced 24.9 fold in the presence of Cd^{2+}. Meanwhile, the fluorescence color of **1O** changed from dark cyan to golden yellow. The binding stoichiometry between **1O** and Cd^{2+} was determined to be 1 : 1. A molecular logic circuit with three inputs and one output was successfully constructed with its light and metal-responsive behaviors. In addition, **1O** was able to selectively recognize HSO_3^- with a 135-fold enhanced fluorescence emission and a notable fluorescence color change from dark cyan to bright cyan. The ^1H NMR and mass spectrometry analyses suggest that the HSO_3^- sensing of **1O** is based on the hydrolysis of the Schiff base group of **1O**.

1. Introduction

Among various heavy metal ions, cadmium(II) is one of the most dangerous ions due to its high toxicity and carcinogenicity.[1,2] As we know, Cd^{2+} has been widely used in many fields such as industry, agriculture, metallurgy, *etc.*[3,4] However, high levels of Cd^{2+} can impose huge threats to the environment and human health due to its bioaccumulation through the food chain.[5,6] Excessive intake of Cd^{2+} can not only increase the risk of cancer, heart disease, cardiovascular diseases and diabetes,[7–10] but also damage the liver and kidneys. As a highly toxic heavy metal, cadmium has been listed on the "CERCLA Priority List of Hazardous Substances" of Toxic Substances and Disease Registry (ATSDR).[11] Thus, efficient methodologies for selective detection of Cd^{2+} are desperately needed. One of the greatest challenges in Cd^{2+} detection is the highly similar binding properties of Cd^{2+} and Zn^{2+} that are located in the same group of the periodic table.[12] Therefore, the development of highly selective sensors of Cd^{2+} without interferences from Zn^{2+} under physiological conditions has become a hot research topic.

Anions play important roles in biological, medical, environmental and chemical sciences.[13–15] Among various anions, bisulfite (HSO_3^-) is one of the most concerned anions, which has been widely used as an enzyme inhibitor, antimicrobial agent, beverages, and an antioxidant for foods.[16] In fact, addition of bisulfite to beer and wine has been customary for centuries in most countries. However, it has been found that some individuals are sensitive to high concentrations of HSO_3^- with the syndromes of asthmatic attack, gastrointestinal distress, allergic reaction and skin allergy.[17–22] Thus, the bisulfite content in foodstuffs has been strictly limited in many countries. For this reason, the selective and sensitive chemosensors of bisulfite are highly desired. To date, many of the reported HSO_3^- sensors have based on different reaction mechanisms, including coordination to metal ions,[23,24] complexation with amines,[25,26] Michael additions,[27–32] selective reaction with aldehyde or levulinate.[33–35] For instance, Zeng *et al.* Reported a mitochondria-targeted probe derived from the conjugation of carbazole and benzo[e]indolium, to which 1,4-nucleophilic addition reaction with bisulfite occurred.[36] However, there are no reports for HSO_3^- sensors, which based on Schiff base with hydrolysis mechanisms.

A variety of advanced technologies, such as inductively coupled plasma-atomic emission spectrometry (ICP-AES),[37] atomic absorption spectroscopy (AAS)[38] and inductively coupled plasma-mass spectrometry (ICP-MS),[39] have been widely used for the analysis of Cd^{2+} and HSO_3^-. By comparison, fluorescent probes are superior and have attracted increasing attentions in ion detections in both chemistry and biology due to their high sensitivity, good selectivity, easy operation, and low cost.[40–46]

Among the reported photo-responsive materials, diarylethene is one of the most promising photo-switchable molecules, which have exhibited great potentials in optical information storage media and photonic switch devices with

Jiangxi Key Laboratory of Organic Chemistry, Jiangxi Science and Technology Normal University, Nanchang 330013, PR China. E-mail: pushouzhi@tsinghua.org.cn; Fax: +86 791 83805870; Tel: +86 791 83805870; +86 791 83831996

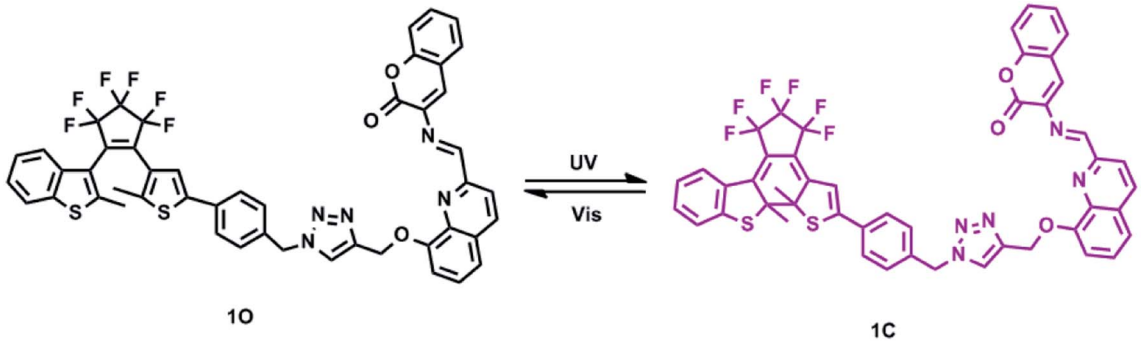

Scheme 1 Photochromism of diarylethene **1O**.

their excellent photo reactivity, thermal stability, and fatigue resistance.[47–51] Moreover, diarylethenes have also been extensively introduced to application in electronic logic devices in recent years, because they exhibit excellent optical performances and multi-response to various ions owing to their special structures.[52–54] As known to all, electronic equipment has gradually become a necessity in people's lives and the logic circuits are essential for the fabrication of optoelectronic devices. According to the above advantages, an increasing number of diarylethenes were introduced to fluorescent sensor for detection of different ions in recent years. For instance, Li *et al.* reported a highly selective fluorescent probe for Cd^{2+} and Zn^{2+} based on a new diarylethene with quinoline–benzimidazole conjugated system,[55] Zhang *et al.* reported a fluorescent sensor for Cd^{2+} based on a new diarylethene with a 1,8-naphthyridine unit,[56] Duan *et al.* studied a fluorescent probe for Cd^{2+} based on a diarylethene with pyridinepiperazine-linked hydroxyquinoline group.[57] However, there are no diarylethene-based chemosensors that exhibit fluorescence response to both Cd^{2+} and HSO_3^-. Thus, development of fluorescent probes toward Cd^{2+} and HSO_3^- are still challenging.

In this study, we designed and synthesized a novel photochromic diarylethene bearing a quinoline-linked 3-aminocoumarin Schiff base unit (**1O**), and its photochromic and fluorescent responses to Cd^{2+} and HSO_3^- were systematically discussed. Scheme 1 shows the photochromic process of **1O**.

2. Experiments

2.1 General methods

All solvents were of analytical grade and distilled before use. Other reagents were used as-received. ^1H NMR and ^{13}C NMR spectra were recorded on a Bruker AV400 spectrometer (400 MHz) using DMSO-d6, $CDCl_3$ and CD_3CN as the solvents and tetramethylsilane (TMS) as the internal standard. Mass spectra were obtained using an Agilent 1100 Ion Trap LC/MS MSD system. Infrared spectra (IR) were collected on a BrukerVertex-70 spectrometer. Melting points were measured using a WRS-1B melting point apparatus. All metal ions, except for Hg^{2+} and K^+ that were prepared with their chloride salts, were obtained by dissolving the corresponding metal nitrates (0.1 mmol) in distilled water (10 mL). All anions were obtained by dissolving the corresponding potassium or sodium salts (0.1 mmol) in distilled water (10 mL). The EDTA solution was prepared with ethylenediaminetetraacetic acid disodium salt (Na_2EDTA) (1.0 mmol) in distilled water (10 mL). Fluorescence spectra were measured with a Hitachi F-4600 fluorescence spectrophotometer. UV-vis absorption spectra were recorded on an Agilent 8453

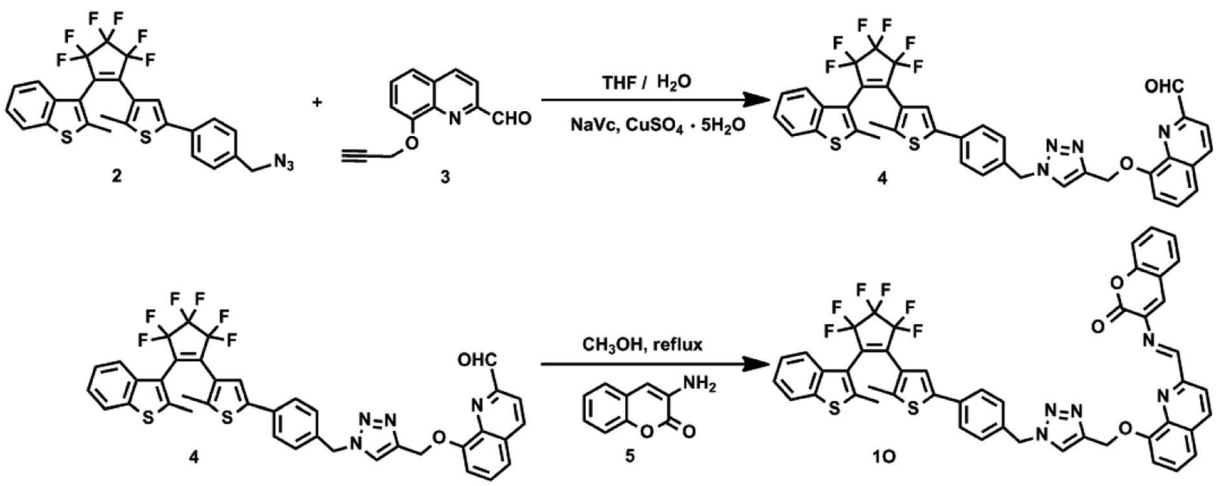

Scheme 2 Synthetic routes of diarylethene **1O**.

UV/vis spectrophotometer equipped with an MUA-165 UV lamp and MVL-210 visible lamp for photoirradiation. Fluorescence quantum yield was measured using a QY C11347-11 absolute PL quantum yield spectrometer. Photoirradiation was conducted on a setup consisting of an SHG-200 UV lamp, Cx-21 ultraviolet fluorescence analysis cabinet, and BMH-250 visible lamp.

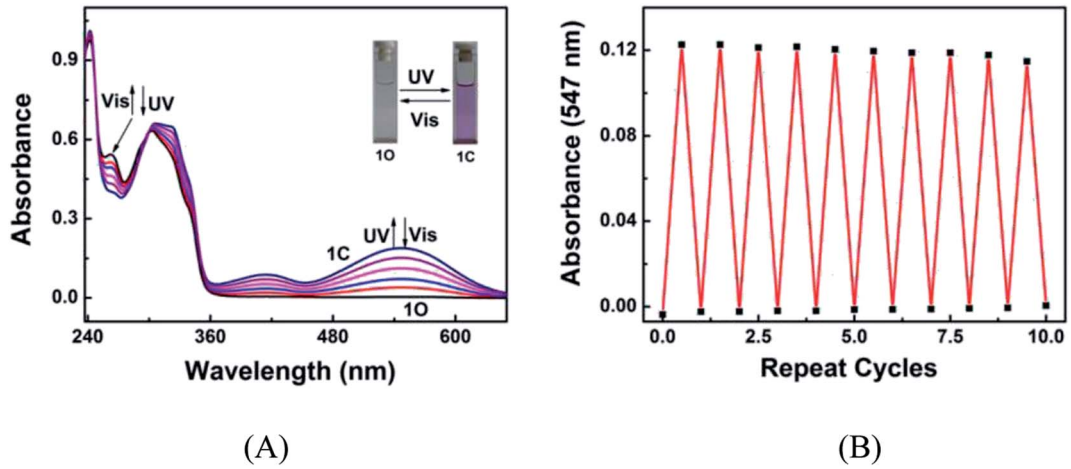

Fig. 1 (A) Changes in the absorption spectrum of **1O** in acetonitrile (2.0×10^{-5} mol L^{-1}) upon alternating irradiation with UV and visible light; (B) fatigue resistance of **1O** in acetonitrile under the alternating irradiation at room temperature.

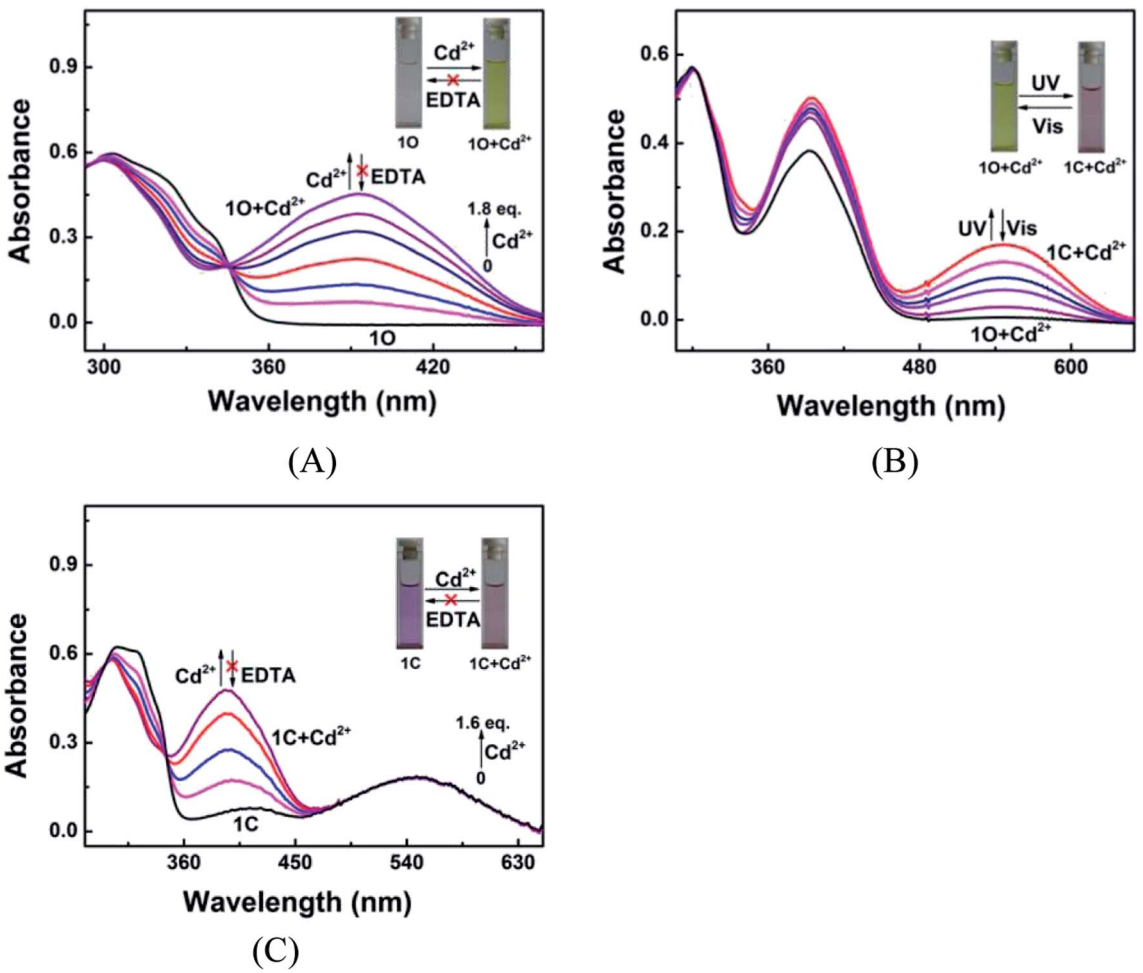

Fig. 2 Changes in the absorption spectrum and color of **1O** in acetonitrile (2.0×10^{-5} mol L^{-1}) in response to Cd^{2+}/EDTA and light stimuli. (A) Spectral changes of **1O** induced by Cd^{2+}/EDTA; (B) spectral changes of **1O** + Cd^{2+} induced by UV/vis light; (C) spectral changes of **1C** induced by Cd^{2+}/EDTA.

2.2 Synthesis of 1O

1O was synthesized following the route shown in Scheme 2. Compounds **2** and **3** were prepared by the methods reported in literature.[58,59]

2.2.1 Synthesis of compound 4. The NaVc (0.04 g, 0.20 mmol) and $CuSO_4$ (0.025 g, 0.10 mmol) solution in water (10 mL) was added to a solution of **2** (0.55 g, 1.00 mmol) and **3** (0.21 g, 1.00 mmol) in THF (40 mL) under stirring at room temperature. The reaction mixture was stirred at room temperature for 12 h to allow the Cu(I)-catalyzed 1,3-dipolar cycloaddition reaction of **2** and **3**, and extracted with CH_2Cl_2. The organic phase was dried over Na_2SO_4, filtered and evaporated. The crude product was purified by silica gel column chromatography using petroleum dichloro/ethyl acetate (v/v = 1/1) as the eluent to afford 0.51 g compound **4** as a purple solid in 67% yield. ^{1}H NMR (400 MHz, $CDCl_3$, ppm): δ 1.94 (s, 3H, $-CH_3$), 2.29 (s, 3H, $-CH_3$), 5.30 (s, 1H, $-CH_2-N-$), 5.52 (s, 2H, $-CH_2-O-$), 5.59 (s, 2H, Ar–H), 7.16 (s, 1H, Ar–H), 7.23 (s, 1H, Ar–H), 7.25 (s, 1H, Ar–H), 7.33 (q, 2H, Ar–H), 7.41 (q, 3H, Ar–H), 7.50 (d, 1H, Ar–H), 7.59 (m, 2H, Ar–H), 7.73 (t, 1H, Ar–H), 8.06 (d, 1H, Ar–H), 8.28 (d, 1H, Ar–H), 10.26 (s, 1H, –CHO).

2.2.2 Synthesis of (1O). Compound **4** (0.23 g, 0.3 mmol) was refluxed with 3-aminocoumarin (0.048 g, 0.3 mmol) in anhydrous methanol (5.0 mL) at 80 °C under stirring for 1 h, cooled to room temperature and filtered. The residue was washed with cold methanol to afford **1O** (0.22 g) in 81% yield. Mp: 439–440 K; ^{1}H NMR (400 MHz, DMSO, ppm): δ 2.35 (s, 3H, $-CH_3$), 3.00 (s, 3H, $-CH_3$), 5.45 (s, 2H, $-CH_2-N-$), 5.72 (s, 2H, $-CH_2-O-$), 6.18 (d, 1H, –CH=N–), 7.15 (s, 1H, Ar–H), 7.29 (d, 1H, Ar–H), 7.35 (t, 3H, Ar–H), 7.40 (s, 1H, Ar–H), 7.42 (s, 2H, Ar–H), 7.47 (q, 2H, Ar–H), 7.52 (s, 1H, Ar–H), 7.54 (s, 1H, Ar–H), 7.60 (q, 2H, Ar–H), 7.62 (s, 1H, Ar–H), 7.79 (d, 1H, Ar–H), 7.94 (d, 1H, Ar–H), 8.51 (d, 2H, Ar–H); ^{13}C NMR (100 MHz, DMSO, TMS): δ = 14.56, 15.07, 50.17, 53.01, 63.50, 83.50, 109.65, 111.73, 116.18, 119.37, 120.60, 120.75, 121.62, 121.92, 123.07, 123.36, 124.59, 124.86, 125.29, 125.71, 125.99, 126.36, 127.07, 127.98, 129.35, 130.98, 132.67, 136.35, 137.81, 138.11, 138.42, 141.20, 142.07, 143.62, 144.23, 148.55, 154.11, 154.52, 159.14; IR (KBr, ν, cm^{-1}): 1715 (–C=O), 1628 (–C=N), 1338 (–C–N), 1275 (–C–O); MS (*m*/*z*): Calculated for $C_{48}H_{31}F_6N_5O_3S_2$ [M]$^+$: 903.1773, found: 904.1836 for [**1O** + H]$^+$ and 926.1658 for [**1O** + Na]$^+$.

3. Results and discussion

3.1 Photochromic of diarylethene 1O

The photochromic behavior of diarylethene **1O** induced by UV/vis light was investigated in acetonitrile (C = 2.0 × 10^{-5} mol L^{-1}) at room temperature. As shown in Fig. 1A, the **1O**

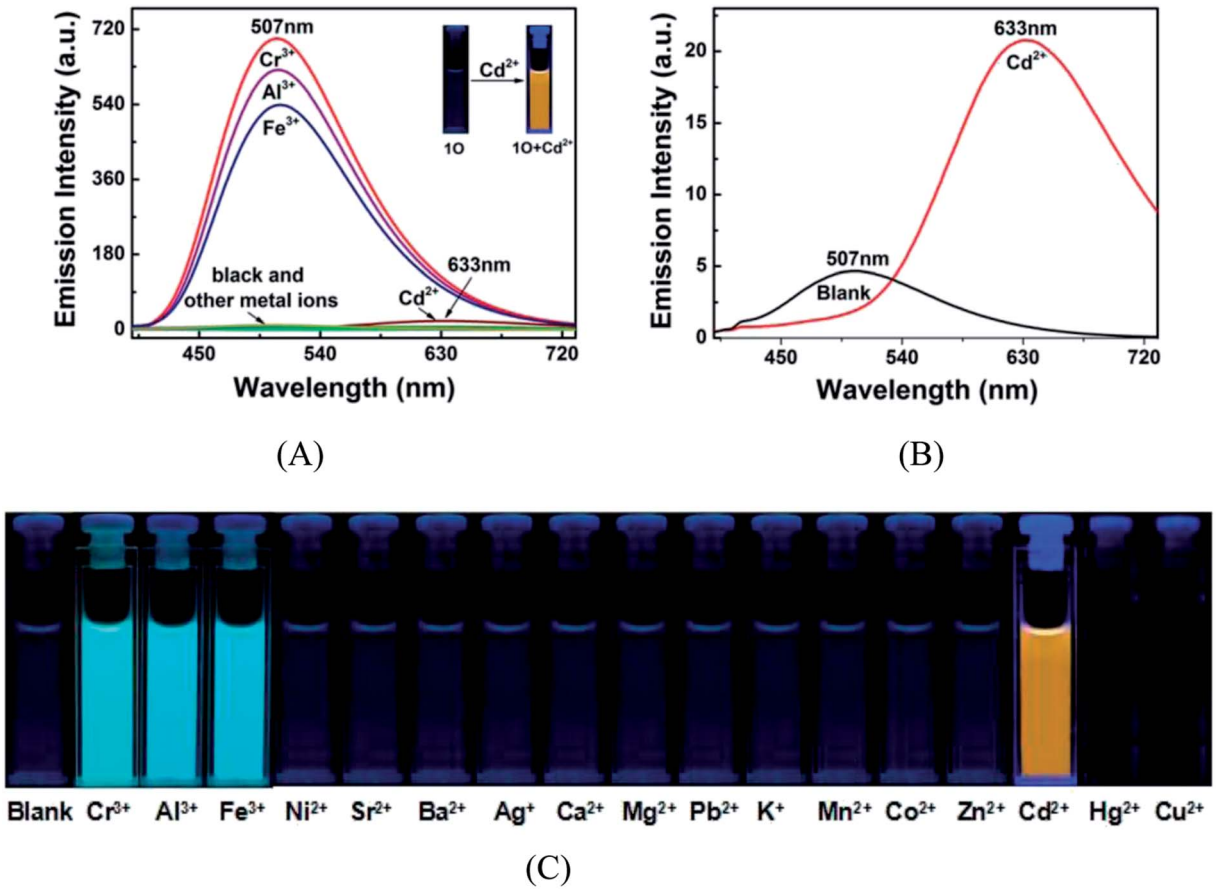

Fig. 3 Fluorescence changes of **1O** (2.0 × 10^{-5} mol L^{-1}) in acetonitrile in response to various metal ions (2.4 equiv.). (A) Fluorescence emission spectra of **1O** in the presence of various metal ions; (B) fluorescence emission spectra of **1O** in the presence of Cd^{2+}; (C) image demonstrating the solution color of **1O** in the presence of different metal ions.

solution in acetonitrile is colorless, exhibiting a sharp absorption peak at 242 nm due to the π–π* transition. A new absorption band centered at 547 nm appeared upon the irradiation with 297 nm light, accompanied with a visible color change from colorless to purple, due to the photocyclization of **1O** to **1C**.[60–62] The photocyclization reaction reached the photostationary state (PSS) in 4.5 min under the irradiation of UV light, where a clear isosbestic point was observed at 300 nm. These observations suggest that the irritation caused a two-component photochromic reaction.[63–65] The absorption spectrum was successfully restored to the original state, accompanied by the color change from purple to colorless, by irradiating the **1C** solution with visible light. The cyclization and cycloreversion quantum yields were calculated to be 0.139 and 0.324, respectively. The fatigue resistance of **1O** was tested by alternating irradiation with UV and visible light at room temperature. Ten coloration–decoloration cycles of **1O** caused only 6.5% degradation (Fig. 1B).

3.2 Changes in absorption spectrum induced by Cd^{2+}

Fig. 2 shows the absorption spectra and colors of **1O** induced by Cd^{2+}/EDTA and UV/vis stimuli in acetonitrile. A new absorption band appeared at 392 nm as Cd^{2+} added and the band intensity increased with the increase of Cd^{2+} amount and reached the maximum at 1.8 equiv. of Cd^{2+}, accompanied by a notable color change from colorless to yellow, due to the formation of complex **1O** + Cd^{2+}. The addition of an excess amount of EDTA did not restore the original color of **1O**, suggesting that the Cd^{2+} sensing process of **1O** was irreversible (Fig. 2A). As depicted in Fig. 2B, the **1O** + Cd^{2+} complex was also photoisomerized under the alternating irradiation with UV and visible light. Upon the irradiation with 297 nm UV light, the yellow solution of **1O** + Cd^{2+} turned plum and a new absorption band emerged at 547 nm ($\varepsilon_{max} = 8.5 \times 10^3$ mol^{-1} L cm^{-1}) due to the formation of the closed-ring isomer **1C** + Cd^{2+}.[66,67] Reversely, the plum solution turned yellow, and the absorption spectrum was restored to that of the open-ring isomer **1O** + Cd^{2+} upon irradiation with visible light. Directly adding Cd^{2+} to the solution of **1C** weakened the absorption band centered at 322 nm and enhanced the absorption at 393 nm. Meanwhile, the solution color changed from purple to plum, indicating that **1C** and Cd^{2+} formed **1C** + Cd^{2+} complex. It is worth noting that the complexation between **1C** and Cd^{2+} was not be reversed by EDTA either (Fig. 2C). These results indicate that both isomers of **1O** have stronger Cd^{2+} binding ability than EDTA.

3.3 Fluorescence response of 1O to metal ions

The fluorescence and color responses of **1O** (2.0×10^{-5} mol L^{-1} in acetonitrile) to various metal cations (2.4 equiv.) including Cd^{2+}, Cr^{3+}, Al^{3+}, Fe^{3+}, Cu^{2+}, Zn^{2+}, Co^{2+}, Mn^{2+}, Hg^{2+}, Pb^{2+}, K^+,

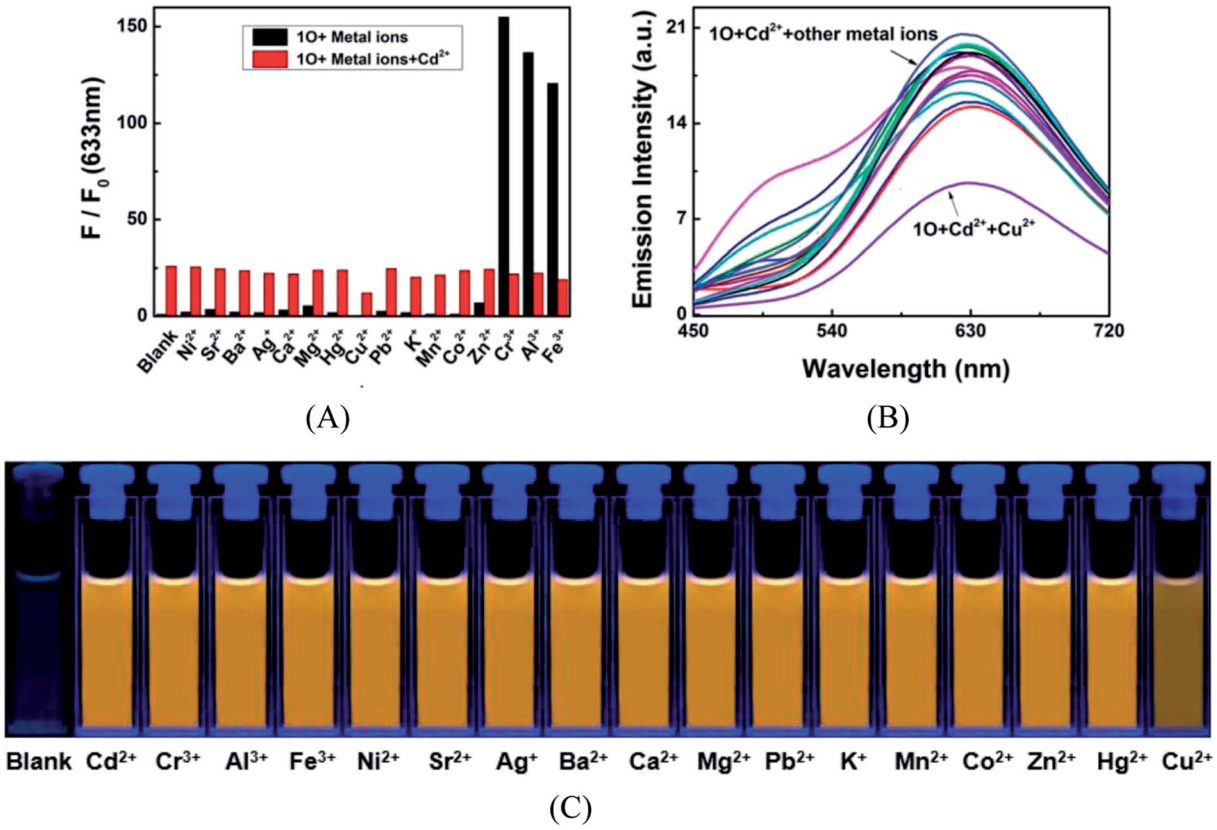

Fig. 4 (A) Competitive tests for the fluorescence response of **1O** (2.0×10^{-5} mol L^{-1}) in the presence of Cd^{2+} and other competing metal ions in acetonitrile. Black bars represent the fluorescence intensities of **1O** in the presence of 2.4 equiv. metal ions. Red bars represent fluorescence intensity of **1O** at 633 nm as in the presence of Cd^{2+} (2.4 equiv.) and other competing metal ions. (B) Emission spectra of **1O** solutions containing Cd^{2+} (2.4 equiv.) and the competing metal ions; (C) fluorescence color of **1O** in the presence of Cd^{2+} and other competing metal ions.

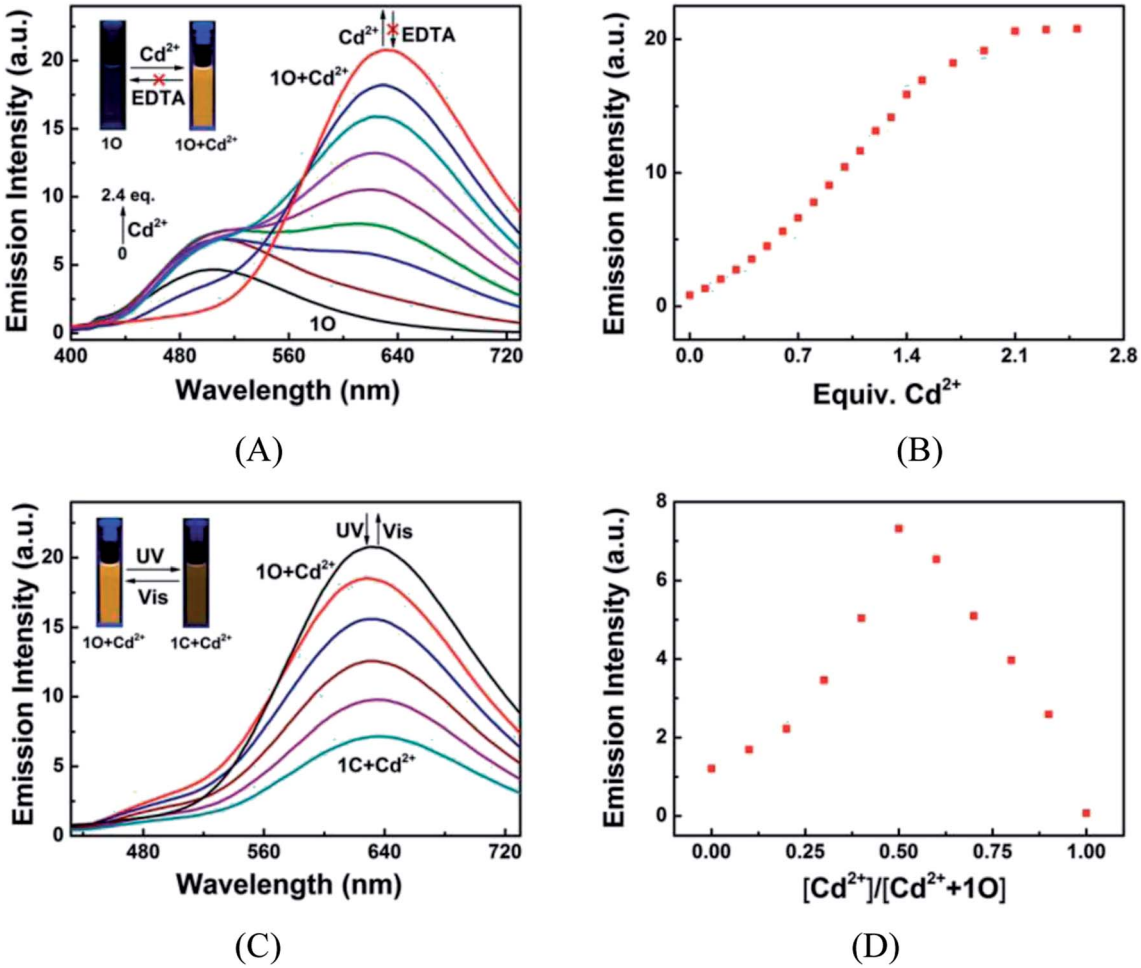

Fig. 5 Fluorescence responses of **1O** (2.0×10^{-5} mol L^{-1}) to Cd^{2+}/EDTA in acetonitrile, excited at 392 nm. (A) Fluorescent emission spectra of **1O** titrated with different amounts of Cd^{2+}; (B) fluorescence intensities of **1O** at 633 nm as titrated with different equiv. of Cd^{2+}; (C) fluorescent emission spectra of **1O** + Cd^{2+} under alternating photoirradiation with UV and visible light; (D) Job's plot showing the 1 : 1 complex of **1O** with Cd^{2+}.

Ca^{2+}, Mg^{2+}, Ba^{2+}, Sr^{2+}, Ag^{+} and Ni^{2+} were investigated with a fluorescence spectroscopy. All metal ions except for Cr^{3+}, Al^{3+} and Fe^{3+} caused no obvious changes in the fluorescence emission at 507 nm of **1O** (Fig. 3A). The fluorescence emission of **1O** at 507 nm was dramatically enhanced as Cr^{3+}, Al^{3+} or Fe^{3+} added, companied by the color change from dark cyan to bright

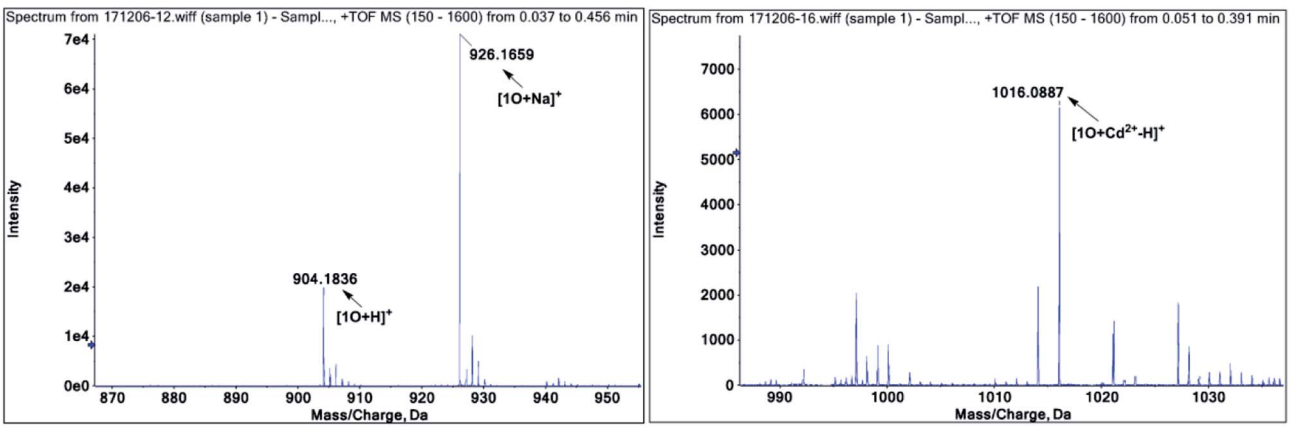

Fig. 6 ESI-MS spectra of **1O** in the absence of presence of Cd^{2+} in acetonitrile.

cyan (Fig. 3C). However, the maximum emission peak had an obvious red-shift from 507 nm to 633 nm upon the addition of Cd^{2+} to **1O** in acetonitrile, we can see this phenomenon more clearly through Fig. 3B. The structural rigidity of the Cd^{2+} complexes and metal binding close to the diarylethene might be the factors that cooperate to induce the large emission peak shift. Meanwhile, it's emission intensity enhanced by 24.9 folds with the stimulation of 2.4 equiv. of Cd^{2+}, accompanied by a color change from dark cyan to golden yellow. These results indicate that **1O** can selectively recognize Cd^{2+} over other metal ions in acetonitrile.

To further demonstrate the selectivity of **1O** towards Cd^{2+} in acetonitrile, competitive experiments were conducted on Cd^{2+} in the presence of equal equivalent of other competitive metal cations listed above. As shown in Fig. 4, the fluorescence response of **1O** to Cd^{2+} was not significantly affected by other competing metal ions, except for Cu^{2+} that caused a reduction in emission intensity. However, compared with the variations of emission intensity and fluorescence color induced by Cd^{2+} alone, the interference of Cu^{2+} is negligible. As mentioned above, most Cd^{2+} fluorescent probes encounter the interference from Zn^{2+} that is located in the same group in the periodic table and has similar chemical properties to Cd^{2+}. Yet such interference was not observed in the Cd^{2+} chemosensing of **1O** too. These results suggested that **1O** is highly selective to Cd^{2+} over other competing cations, even Cr^{3+}, Al^{3+}, Fe^{3+}, and Zn^{2+} in acetonitrile.

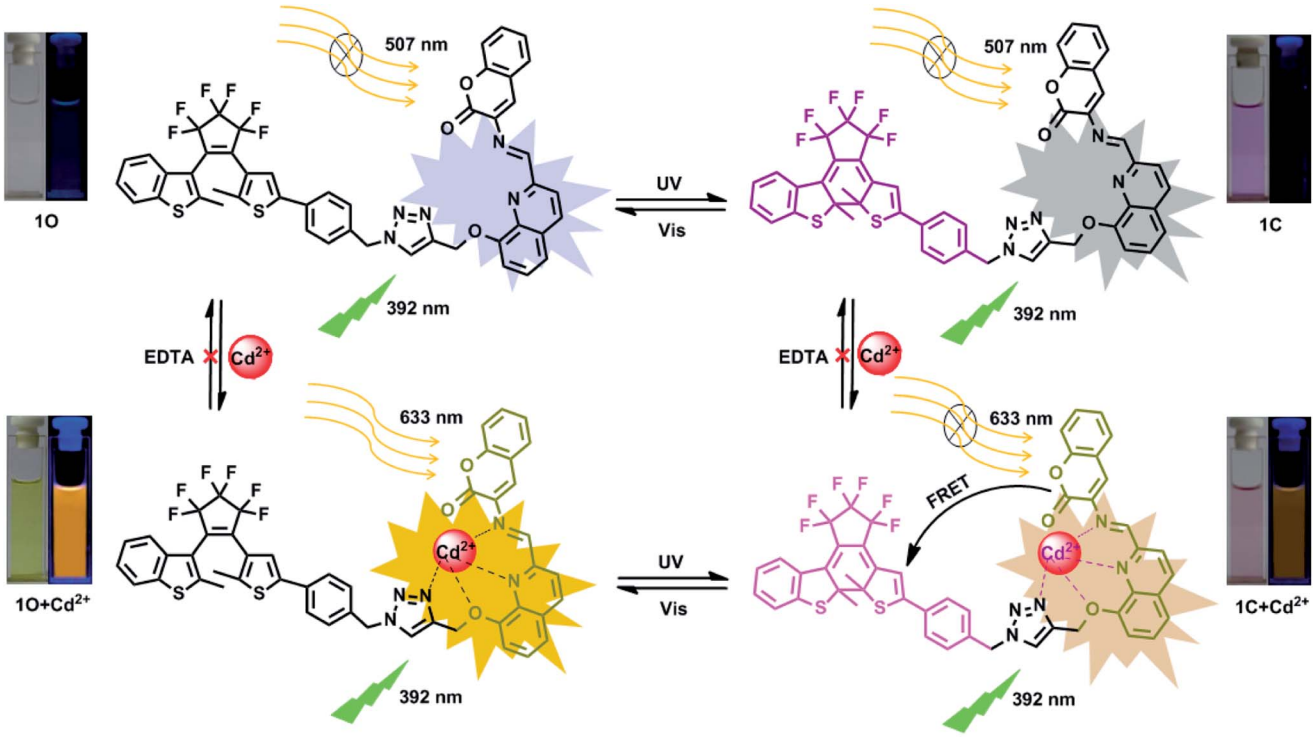

(A)

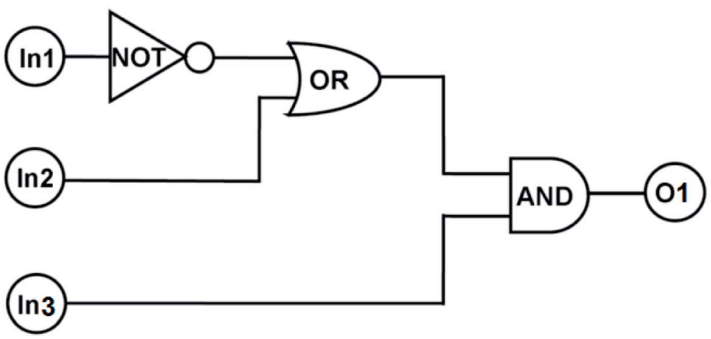

(B)

Fig. 7 (A) Changes in the photochromism, color, and fluorescent of **1O** induced by Cd^{2+}/EDTA and UV/vis lights; (B) the combinational logic circuit equivalents to the truth table in Table 1, where In1 (297 nm UV light), In2 (500 nm visible light), In3 (Cd^{2+}) are inputs, and O1 is output.

Table 1 Truth table for all possible strings of three binary-inputs and the corresponding output digits[a]

Input			
In1 (UV)	In2 (Vis)	In3 (Cd^{2+})	Output λ_{ab} = 393 nm
0	0	0	0
0	0	1	1
1	0	0	0
0	1	0	0
1	0	1	0
0	1	1	1
1	1	0	0
1	1	1	1

[a] The output is defined as 1 if the absorbance at 393 nm is greater than 0.18, otherwise it is defined as 0.

The fluorescence responses of **1O** to Cd^{2+}/EDTA and light stimuli were investigated in acetonitrile at room temperature. The emission peak of **1O** at 507 nm disappeared and a new peak centered at 633 nm appeared as Cd^{2+} added due to the formation of **1O + Cd^{2+}** complex (Fig. 5A). The emission intensity at 633 nm linearly increased with the increase of Cd^{2+} concentration and reached the maximum at 2.4 equiv. Cd^{2+}, followed by a plateau with further titration (Fig. 5B). Meanwhile, the fluorescence color changed from dark cyan to golden yellow. The fluorescence quantum yield of **1O + Cd^{2+}** was determined to be 0.031, 14.5-fold greater than that of **1O** (Φ_f, **1O** = 0.002). The 126 nm re-shift of emission peak and up to 24.9-fold enhanced emission intensity suggest that **1O** is an ideal fluorescent chemosensor of Cd^{2+}. The subsequent addition of excess EDTA did not restore the fluorescence to the original state of **1O**, suggesting that the Cd^{2+} sensing process of **1O** was irreversible. The **1O + Cd^{2+}** complex also exhibited photoswitchable fluorescence behaviors upon alternating irradiation with UV and visible light. The fluorescence of **1O + Cd^{2+}** was quenched dramatically with a clear color change from golden yellow to fawn brown upon the irradiation with 297 nm light, due to the formation of weak fluorescence closed-ring isomer of **1C + Cd^{2+}** (Fig. 5C). However, the fluorescence intensity of **1O + Cd^{2+}** was only reduced to *ca.* 34% at the photostationary state, possibly owing to the incomplete cyclization and the formation of isomers with parallel conformations. The back irradiation with appropriate visible light regenerated the open-ring isomer **1O + Cd^{2+}** and the original emission intensity was recovered.

Additionally, in order to determine the binding stoichiometry between **1O** and Cd^{2+}, the Job's plot with emission intensity at 633 nm as a function of molar fraction of **1O** was drawn. The

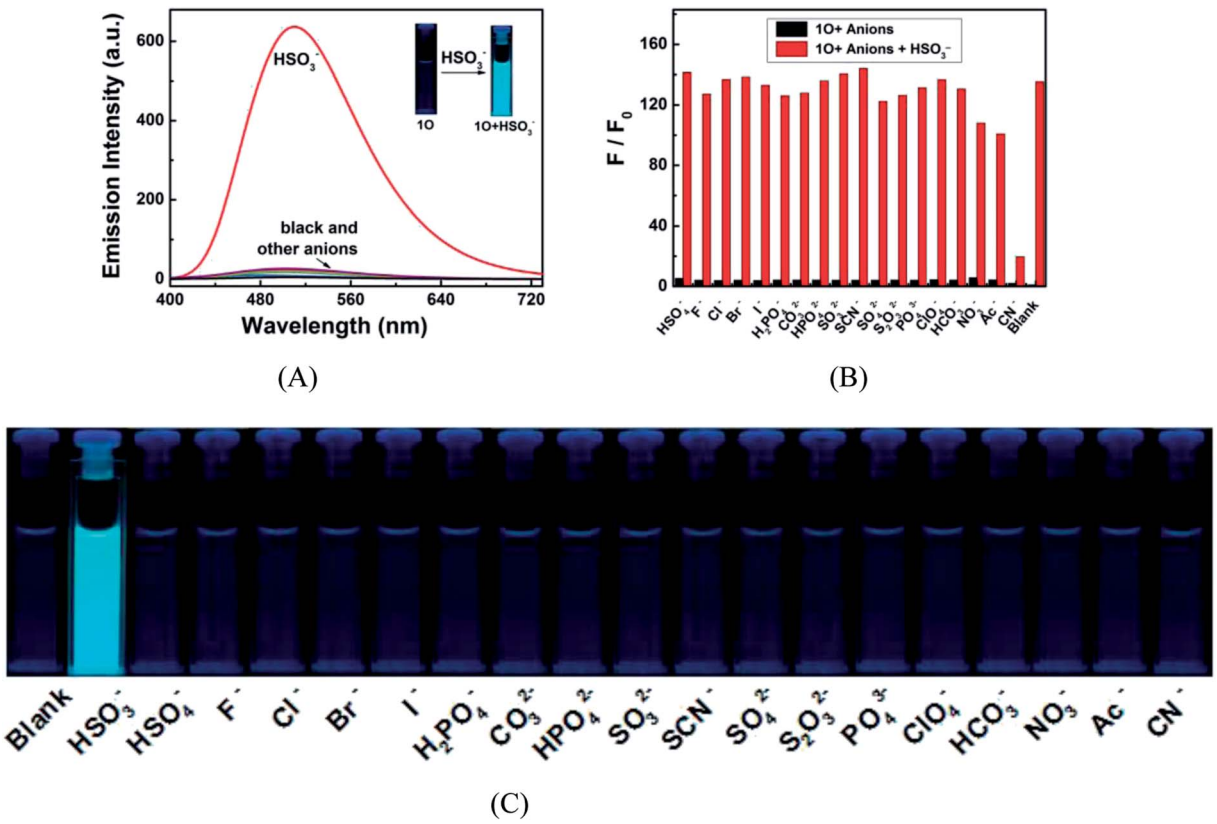

Fig. 8 Fluorescence responses of **1O** (2.0×10^{-5} mol L^{-1} in acetonitrile) to various anions (4.3 equiv.). (A) Fluorescence emission spectra of **1O** in the presence of various anions; (B) competitive experiments for the fluorescence response of **1O** to HSO_3^- and other competing anions in acetonitrile. Black bars represent fluorescence intensities of **1O** in the presence of 4.3 equiv. competing anions. Red bars represent the fluorescence intensities of the corresponding solutions after 4.3 equiv. HSO_3^- added. More details can be found in the web version of this article; (C) fluorescent color of the **1O** solution in the presence of different anions.

concentration of **1O** + Cd^{2+} reached the maximum at the molar fraction of $[Cd^{2+}]/([Cd^{2+}] + [\mathbf{1O}]) = \sim 0.5$ (Fig. 5D), indicating that the binding stoichiometry was 1 : 1. The 1 : 1 coordination stoichiometry of **1O** with Cd^{2+} was further confirmed by the ESI mass spectrometry (ESI-MS) analysis. **1O** exhibited a characteristic peak at 926.1658 *m*/*z* for $[\mathbf{1O} + Na]^+$ (calcd 926.1659) and 904.1836 *m*/*z* for $[\mathbf{1O} + H]^+$ (calcd 904.1852), which disappeared as 2.4 equiv. of Cd^{2+} were added, accompanied by the appearance of a new peak at 1016.0887 *m*/*z* for $[\mathbf{1O} + Cd^{2+} - H]^+$ (calcd 1016.0884) (Fig. 6).

3.4 Application in logic circuits

Based on the photochromic behaviors of the diarylethene **1O** in response to Cd^{2+} and UV/vis lights, a logic circuit was constructed with light irradiations and Cd^{2+} as the inputs and the absorbance of **1O** at 393 nm as the output (Fig. 7). As shown in Fig. 7A, the absorption of **1O** (output) can be effectively modulated by a logic circuit constructed with the three inputs including In1: 297 nm UV light, In2: $\lambda > 500$ nm visible light, and In3: Cd^{2+} (Fig. 7B). The output can be either 'on' or 'off ' with the Boolean value of '1' or '0'. For example, In1 is 'on' with the Boolean value of '1' when 297 nm light is used. Similarly, In2 is '1' as irradiation with appropriate visible light ($\lambda > 500$ nm) is used and In3 is '1' as Cd^{2+} is added. The output is considered at 'on' state with the Boolean value of '1' if the absorbance at 393 nm is greater 0.18. Otherwise, it is regarded at 'off state with the Boolean value of '0'. Table 1 lists all possible strings of the binary inputs and the corresponding output digits. Upon the stimulation of different inputs, the diarylethene can exhibit an on–off–on photochromic switching behavior.

3.5 Fluorescence response of 1O to anions

The fluorescence responses of **1O** to a variety of anions including HSO_3^-, HSO_4^-, F^-, Cl^-, Br^-, I^-, $H_2PO_4^-$, CO_3^{2-}, HPO_4^{2-}, SO_3^{2-}, SCN^-, SO_4^{2-}, $S_2O_3^{2-}$, PO_4^{3-}, ClO_4^-, HCO_3^-, NO_3^-, Ac^- and CN^- were measured in acetonitrile to explore its potential application as a selective anion sensor. As shown in Fig. 8A and C for the fluorescence spectra of **1O** in the presence of 4.3 equiv. anions, none of them, except for HSO_3^- caused notably fluorescent emission at 510 nm and a fluorescent color

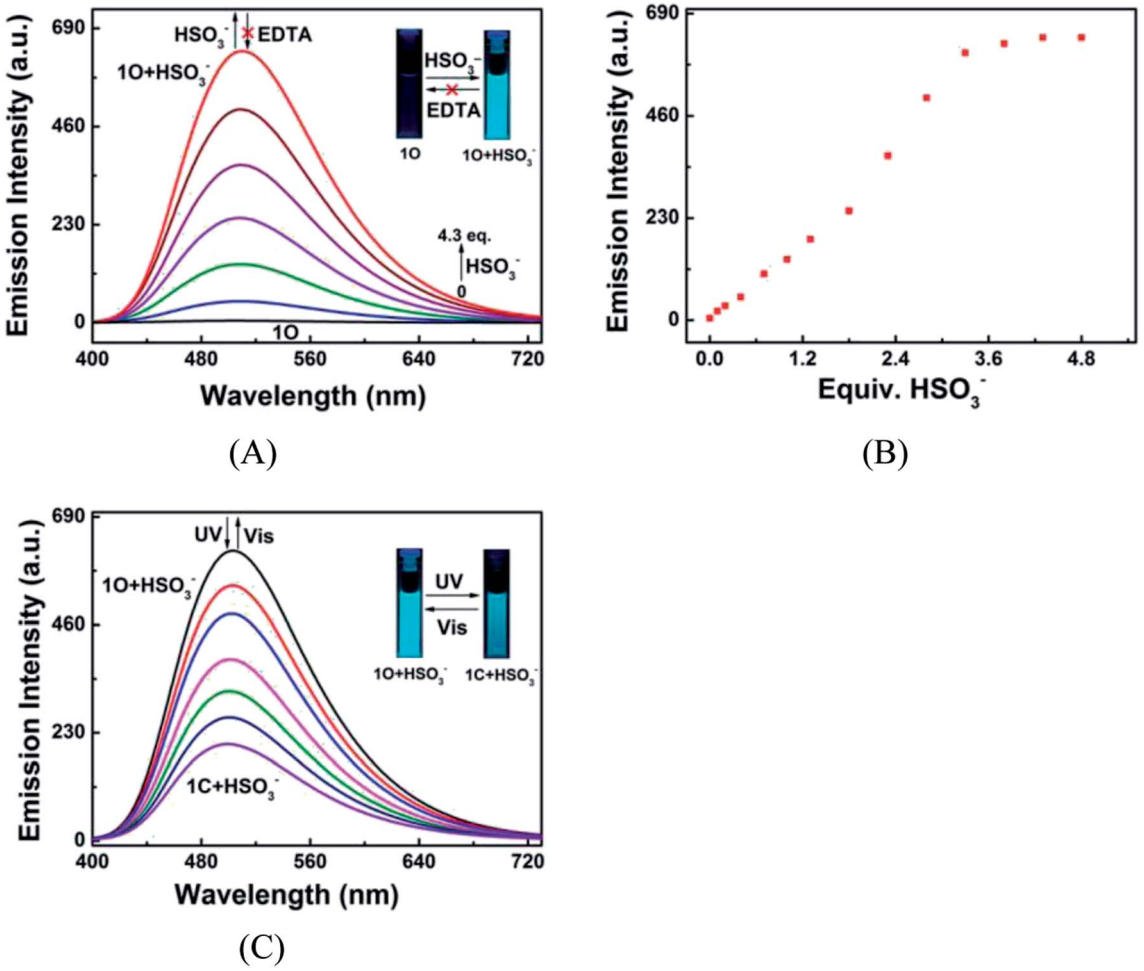

Fig. 9 Changes in the fluorescence of **1O** (2.0×10^{-5} mol L^{-1} in acetonitrile) induced by HSO_3^-/EDTA and light stimuli at room temperature. Excitation: 370 nm. (A) Fluorescence emission spectra of **1O** titrated with different amounts of HSO_3^-; (B) the fluorescence intensities of **1O** at 510 nm in the presence of different equiv. HSO_3^-; (C) fluorescence emission spectra of **1O** + HSO_3^- under the irradiation with UV and visible lights.

change from dark cyan to bright cyan. Compared with that of **1O**, the fluorescence intensity was enhanced by 135.5 folds, suggesting that **1O** can recognize HSO_3^-. The selectivity of the reorganization was further confirmed by competitive experiments. As depicted in Fig. 8B, all competing anions, except for CN^- showed no obvious interference with the HSO_3^- sensing.

To further illuminate the responsive fluorescent emission of **1O** induced by HSO_3^- and UV/vis irradiation, fluorescence titration was conducted at room temperature. As shown in Fig. 9A and B, the fluorescence emission of **1O** at 510 nm linearly increased with the increase of HSO_3^- amount, accompanied by a notable fluorescent color change from dark cyan to bright cyan, and reached the maximum at 4.3 equiv. HSO_3^-, followed by a plateau as HSO_3^- further added. The addition of excess EDTA did not recover its original fluorescence intensity, indicating that the HSO_3^- sensing process of **1O** was

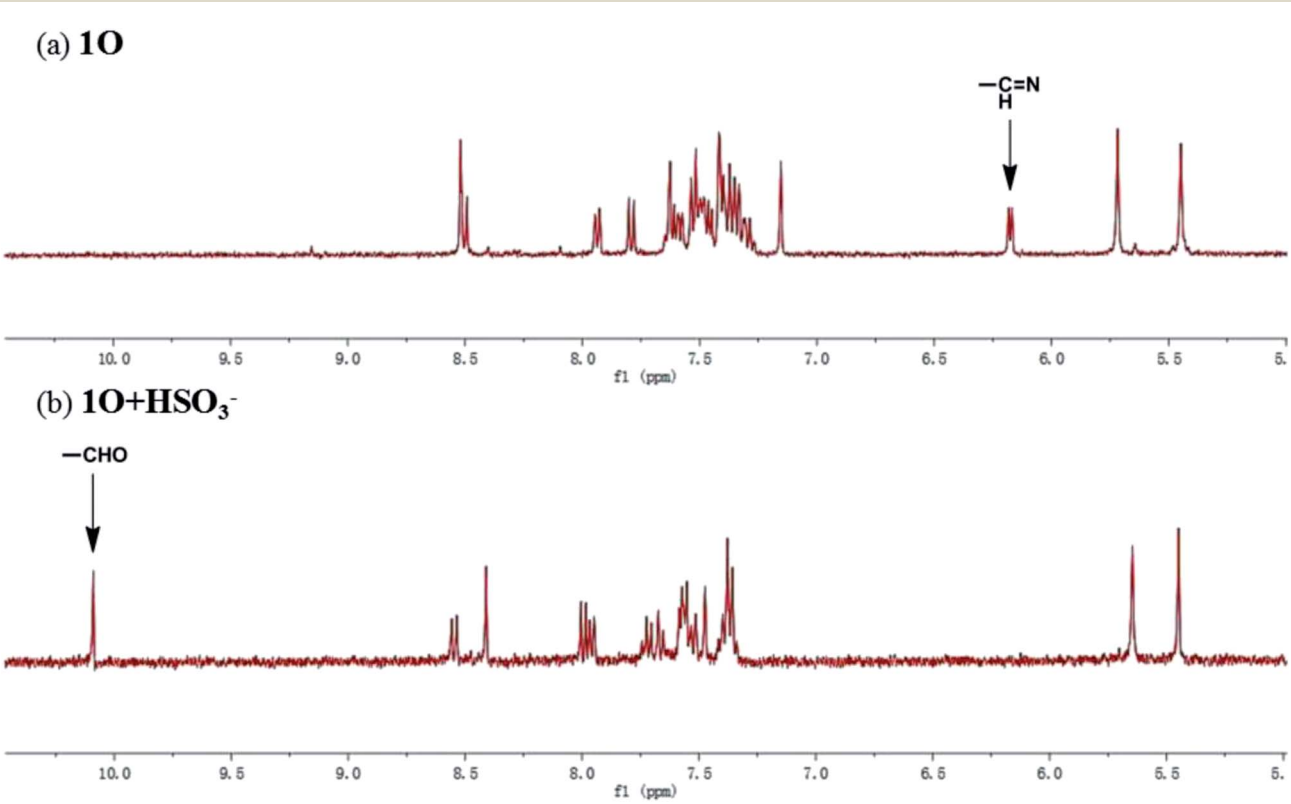

(A)

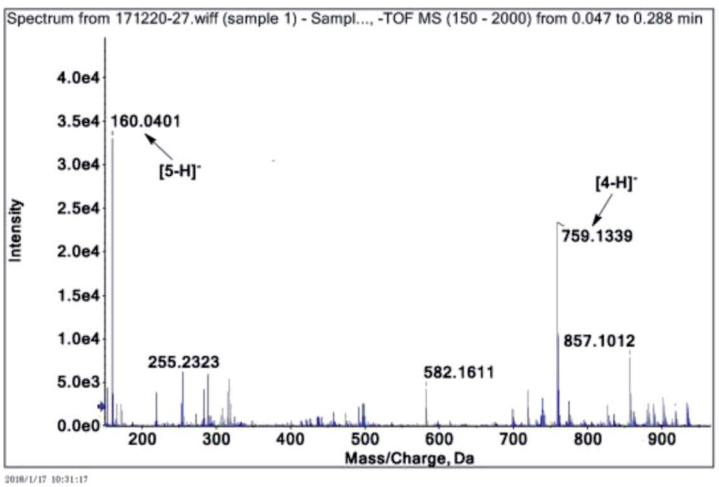

(B)

Fig. 10 (A) Partial ^{1}H NMR spectra of **1O** in the absence (a) and presence of 4.3 eq. (b) of HSO_3^- in deuterated acetonitrile; (B) ESI-MS spectrum of **1O** + HSO_3^-.

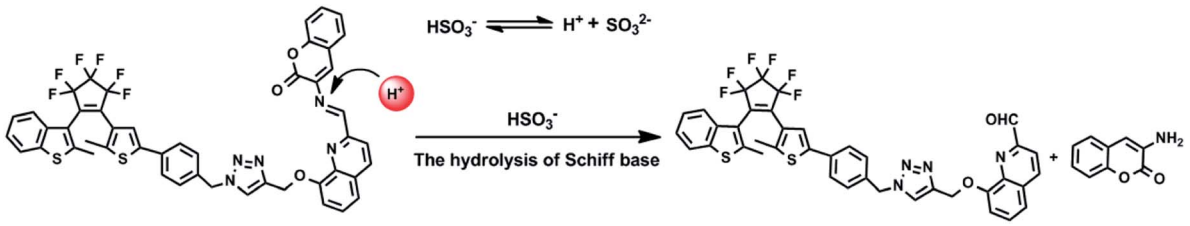

Scheme 3 Possible hydrolysis reaction of **1O** in the presence of HSO_3^- in acetonitrile.

irreversible (Fig. 9A). The absolute fluorescence quantum yield of **1O** + HSO_3^- was determined to be 0.048, 23 folds high than that of **1O** (Φ_f, **1O** = 0.002). These results suggest that the diarylethene can also be potentially used as a fluorescent probe for the quantitative detection of HSO_3^-. The **1O** + HSO_3^- complex also exhibited photoswitchable fluorescence behavior upon alternating irradiation with UV and visible light. The fluorescence of **1O** + HSO_3^- was quenched dramatically with a clear color change from bright cyan to light cyan under the irradiation of 297 nm light, due to the formation of closed-ring isomer **1C** + HSO_3^- (Fig. 9C). The fluorescence intensity of **1O** + HSO_3^- was weakened to *ca.* 32% at PSS due to the incomplete cyclization and existence of isomers with parallel conformations. Upon the irradiation of visible light, the fluorescent spectrum was restored to the initial state of **1O** + HSO_3^-.

To further explore the interaction between **1O** and HSO_3^- in solution and determine the sensing mechanism, the ^{1}H NMR titration of **1O** with HSO_3^- was performed in deuterated acetonitrile. **1O** exhibited a singlet at δ 6.18 ppm of the imine protons (N=CH) (Fig. 10A). As 4.3 equiv. HSO_3^- was added to the **1O** solution, the singlet at δ 6.18 ppm disappeared and a new singlet appeared at δ 10.26 ppm that was attributed to aldehyde protons (–CHO). These results suggest that **1O** was hydrolyzed to afford compound **4** in the presence of HSO_3^- in acetonitrile, similar phenomena were also found in other reported probes.[68–70]

The mass spectra of **1O** and **1O** + HSO_3^- more directly evidenced the reaction. As depicted in Fig. 10B, the peaks of **1O** at 926.1658 *m*/*z* for $[\mathbf{1O} + Na]^+$ (calcd 926.1659) and 904.1836 *m*/*z* for $[\mathbf{1O} + H]^+$ (calcd 904.1852) disappeared after 4.3 equiv. HSO_3^- added, and two new peaks appeared at *m*/*z* = 759.1340 for compound **4**, (calcd $C_{39}H_{26}F_6N_4O_2S_2$ $[M - H]^-$: 759.13216) and 160.0401 for compound **5** (calcd for $C_9H_7NO_2$ $[M - H]^-$: 160.03976). Therefore, the enhanced fluorescence and color change of **1O** in recognizing HSO_3^- was due to the cleavage of imine bond in **1O** that generated aldehyde and amine, *e.g.* compound **4** and 3-aminocoumarin **3**, as depicted in Scheme 3.

4. Conclusion

In summary, a novel photochromic chemosensor, a diarylethene bearing a quinoline-linked 3-aminocoumarin group (**1O**), was designed and synthesized. It exhibited typical photochromism and fluorescent switching properties and high selectivity to Cd^{2+} and HSO_3^-. **1O** showed a straightforward response for the selective detection of Cd^{2+}, ~126 nm red shifted emission peak and up to 24.9-fold enhanced fluorescence intensity, accompanied by a notable fluorescent color change from dark cyan to golden yellow. The competitive experiments suggest that such selective fluorescent response of **1O** to Cd^{2+} is not interfered by other competing metal cations including Zn^{2+}. The binding stoichiometry between **1O** and Cd^{2+} was determined to be 1 : 1. Similarly, it was found that HSO_3^- was able to enhance the fluorescence emission of **1O** in acetonitrile up to 135.5-fold and caused a notable fluorescence color change from dark cyan to bright cyan due to the hydrolysis of the C=N bond in **1O** that produced an aldehyde and amine. These results suggest that the diarylethene derivative has a great application potential as a fluorescent sensor of both Cd^{2+} and HSO_3^-.

Conflicts of interest

There are no conflicts of interest to declare.

Acknowledgements

The authors are grateful for the financial support from the National Natural Science Foundation of China (21363009, 21662015), the "5511" science and technology innovation talent project of Jiangxi, the key project of Natural Science Foundation of Jiangxi Province (20171ACB20025), the Science Funds of Natural Science Foundation of Jiangxi Province (20171BAB203014, 20171BAB203011).

References

1 L. Zhang, W. Hu, L. Yu and Y. Wang, *Chem. Commun.*, 2015, **51**, 4298–4301.
2 Z. Shi, Q. Han, L. Yang, H. Yang, X. Tang, W. Dou, *et al.*, *Chem.–Eur. J.*, 2015, **21**(1), 290–297.
3 S. F. Zhou, J. J. Wang, L. Gan, X. J. Han, H. L. Fan, L. Y. Mei, J. Huang and Y. Q. Liu, *J. Alloys Compd.*, 2017, **721**, 492–500.
4 R. Kumar, T. Bhuvana and A. Sharma, *RSC Adv.*, 2017, **7**, 42146–42158.
5 J. N. Hao and B. Yan, *Chem. Commun.*, 2015, **51**, 7737–7740.
6 Y. Lv, L. Wu, W. Shen, J. Wang, G. Xuan and X. Sun, *J. Porphyrins Phthalocyanines*, 2015, **19**, 769–774.
7 C. D. Klaassen, J. Liu and B. Diwan, *Toxicol. Appl. Pharmacol.*, 2009, **238**, 215–220.
8 X. Y. Xu and B. Yan, *Sens. Actuators, B*, 2016, **222**, 347–353.

9 Y. Luo, D. Tang, W. Zhu, Y. Xu and X. Qian, *J. Mater. Chem. C*, 2015, **3**, 8485–8489.
10 V. N. Mehta, J. V. Rohit and S. K. Kailasa, *New J. Chem.*, 2016, **40**, 4566–4574.
11 Agency for Toxic Substances and Disease Registry, 4770 Buford Hwy NE, Atlanta, GA 30341, http://www.atsdr.cdc.gov/cercla/07list.html.
12 A. Sil, A. Maity, D. Giri and S. K. Patra, *Sens. Actuators, B*, 2016, **226**, 403–411.
13 J. J. Park, Y. H. Kim, C. Kim and J. Kang, *Tetrahedron Lett.*, 2011, **52**, 2759–2763.
14 H. Li, *Anal. Chim. Acta*, 2015, **897**, 102–108.
15 J. Y. Noh, I. H. Hwang, H. Kim, E. J. Song, K. B. Kim and C. Kim, *Bull. Korean Chem. Soc.*, 2013, **34**, 1985.
16 M. Li, W. Feng, H. Zhang and G. Feng, *Sens. Actuators, B*, 2017, **243**, 51–58.
17 G. Xu, H. Wu, X. Liu, R. Feng and Z. Liu, *Dyes Pigm.*, 2015, **120**, 322–327.
18 D. P. Li, Z. Y. Wang, X. J. Cao, J. Cui, X. Wang, H. Z. Cui, J. Y. Miao and B. X. Zhao, *Chem. Commun.*, 2016, **52**, 2760–2763.
19 Y. Zhang, L. Guan, H. Yu, Y. Yan, L. Du, Y. Liu, M. Sun, D. Huang and S. Wang, *Anal. Chem.*, 2016, **88**, 4426–4431.
20 J. Xu, J. Pan, X. Jiang, C. Qin, L. Zeng, H. Zhang and J. Zhang, *Biosens. Bioelectron.*, 2016, **77**, 725–732.
21 W. L. Wu, Z. Y. Wang, X. Dai, J. Y. Miao and B. X. Zhao, *Sci. Rep.*, 2016, **6**, 25315.
22 G. Wang, H. Chen, X. Chen and Y. Xie, *RSC Adv.*, 2016, **6**, 18662–18666.
23 L. He, W. Lin, Q. Xu and H. Wei, *ACS Appl. Mater. Interfaces*, 2014, **6**, 22326–22333.
24 L. Yuan, W. Lin, K. Zheng, L. He and W. Huang, *Chem. Soc. Rev.*, 2013, **42**, 622–661.
25 A. V. Leontiev and D. M. Rudkevich, *J. Am. Chem. Soc.*, 2005, **127**, 14126–14127.
26 Y. Sun, C. Zhong, R. Gong, H. Mu and E. Fu, *J. Org. Chem.*, 2009, **74**, 7943–7946.
27 Q. Sun, W. Zhang and J. Qian, *Talanta*, 2017, **162**, 107–113.
28 Y. Chen, X. Wang, X. Yang, Y. Zhong, Z. Li and H. Li, *Sens. Actuators, B*, 2015, **206**, 268–275.
29 W. Chen, Q. Fang, D. Yang, H. Zhang, X. Song and J. Foley, *Anal. Chem.*, 2015, **87**, 609–616.
30 J. Xu, J. Pan, X. Jiang, C. Qin, L. Zeng, H. Zhang, *et al.*, *Biosens. Bioelectron.*, 2016, **77**, 725–732.
31 M. J. Peng, X. F. Yang, B. Yin, Y. Guo, F. Suzenet, D. En and Y. W. Duan, *Chem.–Asian J.*, 2014, **9**, 1817–1822.
32 L. Tan, W. Lin, S. Zhu, L. Yuan and K. Zheng, *Org. Biomol. Chem.*, 2014, **12**, 4637–4643.
33 L. M. Zhu, J. C. Xu, Z. Sun, B. Q. Fu, Q. Q. Qin, L. T. Zeng, *et al.*, *Chem. Commun.*, 2015, **5**, 1154–1156.
34 X. Liu, Q. Yang, W. Chen, L. Mo, S. Chen, J. Kang, *et al.*, *Org. Biomol. Chem.*, 2015, **13**, 8663–8668.
35 S. Yu, X. Yang, Z. Shao, Y. Feng, X. Xi, R. Shao, *et al.*, *Sens. Actuators, B*, 2016, **235**, 362–369.
36 J. Xu, J. Pan, X. Jiang, C. Qin, L. Zeng, H. Zhang, *et al.*, *Biosens. Bioelectron.*, 2016, **77**, 725–732.
37 D. P. Li, Z. Y. Wang, X. J. Cao, J. Cui, X. Wang, H. Z. Cui, J. Y. Miao and B. X. Zhao, *Chem. Commun.*, 2016, **52**, 2760–2763.
38 F. Sa, W. T. Vong, T. M. Chan and C. W. K. Lam, *Clin. Chim. Acta*, 2010, **411**, 909.
39 M. A. Hamilton, P. W. Rode, M. E. Merchant and J. Sneddon, *Microchem. J.*, 2008, **88**, 52–55.
40 Y. X. Zuo, J. K. Xu, F. X. Jiang, X. M. Duan, L. M. Lu, G. Ye, C. C. Li and Y. F. Yu, *J. Electroanal. Chem.*, 2017, **794**, 71–77.
41 Y. Yue, F. Huo, C. Yin, J. O. Escobedo and R. M. Strongin, *Analyst*, 2016, **141**, 1859–1873.
42 T. Kowada, H. Maed and K. Kikuchi, *Chem. Soc. Rev.*, 2015, **44**, 4955–4972.
43 H. D. Xiao, K. Xin, H. F. Dou, G. Yin, Y. W. Quan and R. Y. Wang, *Chem. Commun.*, 2015, **51**, 1442–1445.
44 W. W. Qin, W. Dou, V. Leen, W. Dehaen, M. V. D. Auweraer and N. Boens, *RSC Adv.*, 2016, **6**, 7806–7816.
45 B. Sen, M. Mukherjee, S. Banerjee, S. A. Pal and P. Chattopadhyay, *Dalton Trans.*, 2015, **44**, 8708–8717.
46 Q. Lin, T. T. Lu, X. Zhu, T. B. Wei, H. Li and Y. M. Zhang, *Chem. Sci.*, 2016, **7**, 5341–5346.
47 M. Irie, T. Fukaminato and K. Matsuda, *Chem. Rev.*, 2014, **114**, 12174–12277.
48 W. L. Li, X. Li, Y. S. Xie, Y. Wu, M. Q. Li, X. Y. Wu, *et al.*, *Sci. Rep.*, 2015, **5**, 9186.
49 G. T. Xu, B. Li, J. Y. Wang, D. B. Zhang and Z. N. Chen, *Chem.–Eur. J.*, 2015, **21**, 3318–3326.
50 B. Li, H. M. Wen, J. Y. Wang, L. X. Shi and Z. N. Chen, *Inorg. Chem.*, 2015, **54**, 11511–11519.
51 Y. L. Fu, Y. Y. Tu, C. B. Fan, C. H. Zheng, G. Liu and S. Z. Pu, *New J. Chem.*, 2016, **40**, 8579–8586.
52 S. Z. Pu, Q. Sun, C. B. Fan, R. J. Wang and G. Liu, *J. Mater. Chem. C*, 2016, **4**, 3075–3093.
53 S. J. Xia, G. Liu and S. Z. Pu, *J. Mater. Chem. C*, 2015, **3**, 4023–4029.
54 G. Li, L. L. Ma, G. Liu, C. B. Fan and S. Z. Pu, *RSC Adv.*, 2017, **7**, 20591.
55 G. Li, D. B. Zhang, G. Liu and S. Z. Pu, *Tetrahedron Lett.*, 2016, **57**, 5205–5210.
56 X. X. Zhang, R. J. Wang, C. B. Fan, G. Liu and S. Z. Pu, *Dyes Pigm.*, 2017, **139**, 208–217.
57 F. Duan, G. Liu, P. Liu, C. B. Fan and S. Z. Pu, *Tetrahedron*, 2016, **72**, 3213–3220.
58 G. F. Wu, M. X. Li, J. J. Zhu, K. W. C. Lai, Q. X. Tong and F. Lu, *RSC Adv.*, 2016, **6**, 100696–100699.
59 S. Z. Pu, H. C. Ding, G. Liu, C. H. Zheng and H. Y. Xu, *J. Phys. Chem. C*, 2014, **118**, 7010–7017.
60 C. B. Fan, L. L. Gong, L. Huang, F. Luo, R. Krashina, X. F. Yi, *et al.*, *Angew. Chem., Int. Ed.*, 2017, **56**, 7900–7906.
61 S. Y. Li, D. B. Zhag, J. Y. Wang, R. M. Lu, C. H. Zheng and S. Z. Pu, *Sens. Actuators, B*, 2017, **245**, 263–272.
62 S. L. Guo, G. Liu, C. B. Fan and S. Z. Pu, *Sens. Actuators, B*, 2018, **266**, 603–613.
63 S. Z. Pu, C. C. Zhang, C. B. Fan and G. Liu, *Dyes Pigm.*, 2016, **129**, 24–33.
64 H. J. Jia, S. Z. Pu, C. B. Fan, G. Liu and C. H. Zheng, *Dyes Pigm.*, 2015, **121**, 211–220.

65 H. C. Ding, B. Q. Lia, S. Z. Pu, G. Liu, D. C. Jia and Z. Yu, *Sens. Actuators, B*, 2017, **247**, 26–35.
66 E. T. Feng, C. B. Fan, N. S. Wang, G. Liu and S. Z. Pu, *Dyes Pigm.*, 2018, **151**, 22–27.
67 Z. L. Shi, Y. Y. Tu, R. J. Wang, G. Liu and S. Z. Pu, *Dyes Pigm.*, 2018, **149**, 764–773.
68 L. Y. Wang, J. J. Ou, G. P. Fang and D. R. Cao, *Sens. Actuators, B*, 2016, **222**, 1184–1192.
69 Z. L. Luo, K. Yin, Z. Yu, M. X. Chen, Y. Li and J. Ren, *Spectrochim. Acta, Part A*, 2016, **169**, 38–44.
70 S. Erdemir, B. Tabakci and M. Tabakci, *Sens. Actuators, B*, 2016, **228**, 109–116.